Journal of Power Sources 246 (2014) 90–94

Contents lists available at ScienceDirect

Journal of Power Sources

journal homepage: www.elsevier.com/locate/jpowsour

Short communication

Analysis of the behavior and degradation in proton exchange membrane fuel cells with a dead-ended anode

Jianliang Yu [a], Zuwei Jiang [a], Ming Hou [b,*], Dong Liang [c], Yu Xiao [b], Meiling Dou [b,d], Zhigang Shao [b,1], Baolian Yi [b]

[a] School of Chemical Machinery, Dalian University of Technology, Dalian 116024, Liaoning, China
[b] Fuel Cell System and Engineering Laboratory, Dalian Institute of Chemical Physics, Chinese Academy of Sciences, Dalian 116023, China
[c] Sunrise Power Co., Ltd, Dalian 116085, China
[d] Graduate University of Chinese Academy of Sciences, Beijing 100049, China

HIGHLIGHTS

- Local current firstly degrades at anode outlet region, then proceeds to the inlet.
- The fuel starvation leads to a high cathode potential and carbon corrosion.
- SEM images reveal thickness reduction and porous structure collapse.
- The dominant factor, leading to the performance decay, is the nitrogen crossover.

ARTICLE INFO

Article history:
Received 20 November 2012
Received in revised form
27 June 2013
Accepted 28 June 2013
Available online 8 July 2013

Keywords:
Proton exchange membrane fuel cell
Hydrogen depleted region
Dead-ended anode
Current distribution
Local potential

ABSTRACT

Proton exchange membrane fuel cells (PEMFCs) with a dead-ended anode (DEA) can obtain high hydrogen utilization by a comparatively simple system. Nevertheless, the accumulation of the nitrogen and the water in the anode channels can lead to a local fuel starvation, which degrades the performance and durability of PEMFCs. In this paper, the behaviors of PEMFCs with a DEA are explored experimentally by detecting the current distribution and the local potentials. The results indicate that the current distribution is uneven during the DEA operation. The local current firstly decreases at the region near the anode outlet, and then extends to the inlet region along the channels with time. The complete fuel starvation near the anode outlet leads to a high local potential and carbon corrosion on the cathode side. The SEM images of the cathode electrode reveal that the significant thickness reduction and the collapse of the electrode's porous structure happen in the cathode catalyst layer, leading to the irreversible decline of the performance. The comparison of the experiments with different oxidants and fuels reveals that the nitrogen crossover from cathode to anode is the dominant factor on the performance decline under the DEA operations.

© 2013 Elsevier B.V. All rights reserved.

1. Introduction

Proton exchange membrane fuel cells (PEMFCs) have been considered as a potential alternative to conventional internal combustion engines due to the low operation temperature, fast response, near-zero emissions and favorable power-to-weight ratio. However, several technical issues still prevent the further applications of fuel cells, such as the low hydrogen utilization and the complex system. Under the dead-end anode (DEA) operation, hydrogen is supplied for the reactions on demand by a pressure regulator. Thus, the PEMFCs can obtain high hydrogen utilization. However, when air is employed as the oxidant, the water vapor and inert nitrogen can also crossover the membrane due to the concentration gradients between the anode and cathode [1–4], which results in the local fuel starvation and subsequently carbon corrosion [3,5–7]. Siegel et al. [4] employed neutron images to investigate the liquid water accumulation in a PEMFC with a DEA. Even dry hydrogen was supplied to the anode, the accumulation of liquid water could be still observed in the anode channels in normal operation conditions. The accumulations of water and nitrogen lead to the uneven distribution of the fuel gas. Sasmito et al. [3] and

* Corresponding author. Tel.: +86 411 84379051; fax: +86 411 84379185.
E-mail addresses: houming@dicp.ac.cn (M. Hou), zhgshao@dicp.ac.cn (Z. Shao).
[1] Tel.: +86 411 84379153; fax: +86 411 84379185.

0378-7753/$ – see front matter © 2013 Elsevier B.V. All rights reserved.
http://dx.doi.org/10.1016/j.jpowsour.2013.06.163

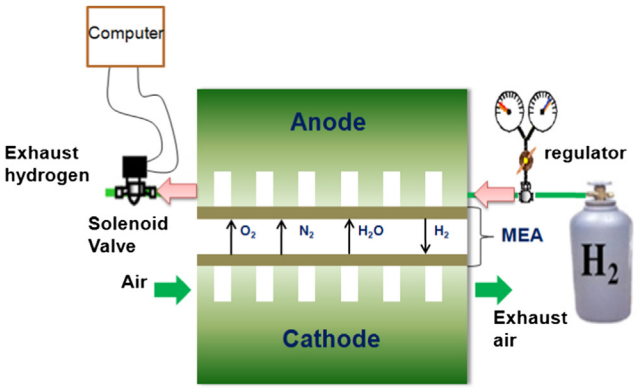

Fig. 1. Schematic of the experimental setup.

Siegel et al. [5] presented models to describe the dynamic evolution of the species in the anode channel and predicted the voltage decline during the purge cycles. Baumgartner et al. [6] adopted a laboratory-scale single cell assembly with four reference electrodes (RHEs) to investigate the electrode potentials under the dead-ended operation. The evolutions of the anode and cathode potentials exhibited that the fuel starvation and carbon corrosion occurred under the DEA operation. The corrosion of carbon support layer was confirmed by the presence of CO_2 in the cathode. Chen et al. [7] developed an along-channel model to predict the carbon corrosion in a PEMFC with a DEA. The model captured the effect of nitrogen accumulation and the current density distribution on the carbon loss, and then predicted the non-recoverable voltage loss. Instructive results were given in the above work, but the irregular distributions of local current density and the corrosion process of PEMFC with a DEA were seldom experimentally investigated.

In this paper, the current distribution, the local potentials, and the catalyst layer micro-structure are measured in order to well understand the PEMFC behaviors under the DEA operation. The degradation mechanism of the PEMFC with a DEA is further analyzed.

2. Experimental

A single cell with the active area of 270 cm^2 was used in the research. Dry hydrogen was fed via a pressure regulator. A solenoid valve was placed at the outlet of the anode for purging control, as shown in Fig. 1. The periodic purging event causes voltage cycling in DEA operation, with a cycle defined as the duration between two consecutive purge events. The tested fuel cell was laid on its side as shown in Fig. 2. A special cathode current collecting end-plate was adopted to measure the current distribution. The end-plate was segmented by embedding fifteen graphite blocks in a plexiglass plate and uniformly arranged in a matrix of 3 × 5. The area of each graphite block was 15.36 cm^2. The segments, which consisted of three parallel graphite blocks perpendicularly to hydrogen flow direction, were also numbered from 5 to 1 along the hydrogen flow direction (see Fig. 2). The flow fields of both cathode and anode were parallel-straight channels. The width and depth of each channel are both 1 mm, with the ratio of channel to rib 1:1 [8].

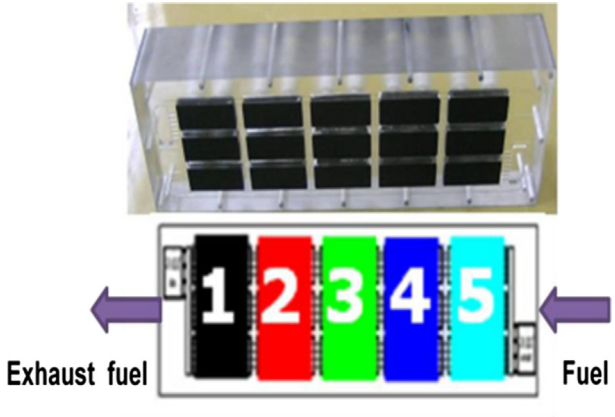

Fig. 2. Schematic of the cathode end-plate.

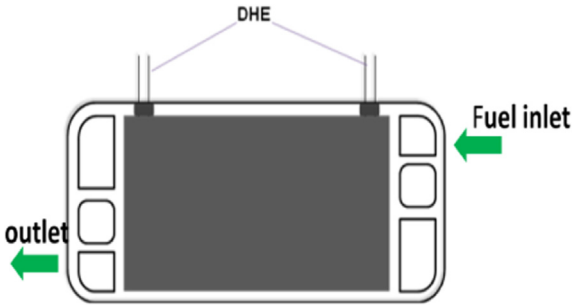

Fig. 3. Schematic of the MEA with DHE.

The dynamic hydrogen reference electrodes (DHEs), which were similar to the design of Siroma et al. [9], were embedded in the membrane electrode assembly (MEA) to measure the local potentials. The DHEs were arranged at the anode inlet and outlet region, as shown in Fig. 3. The local potentials were recorded simultaneously. The applied MEA consisted of five layers: the Nafion® 212 membrane in the middle, and two catalyst layers (CLs) and gas diffusion layers (GDLs) on both sides. The Pt loading of CLs at each side was 0.4 mg cm^{-2}. The GDL included the carbon paper (Toray, TGP-H-060) and a micro pore layer (MPL); and its thickness was about 0.2 mm. In the experiments, the operating conditions of the fuel cells were controlled by the G100 fuel cell test station from Green light Innovation Corp of Canada.

3. Results and discussion

3.1. Local current distribution

The fuel cell interior current distribution was measured by the potentiostatic method. The air flux was fixed at 5.61 L min^{-1}, with

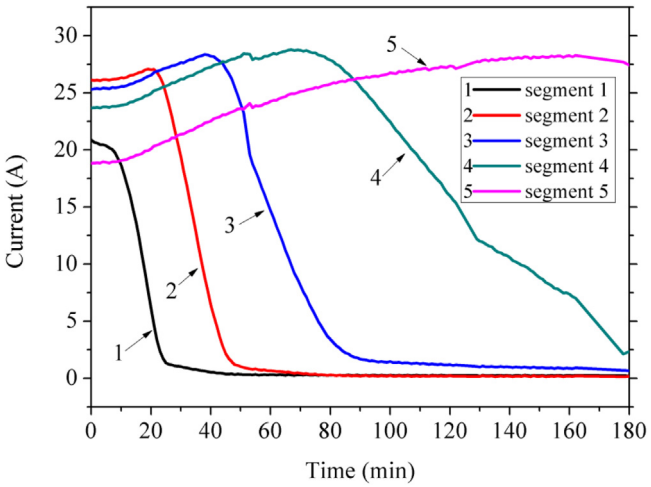

Fig. 4. Evolution of the current distribution.

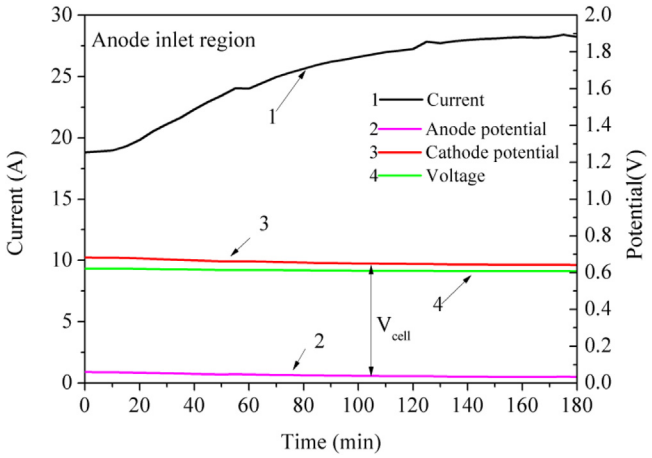

Fig. 5. Evolution of local potential and current at the anode inlet region.

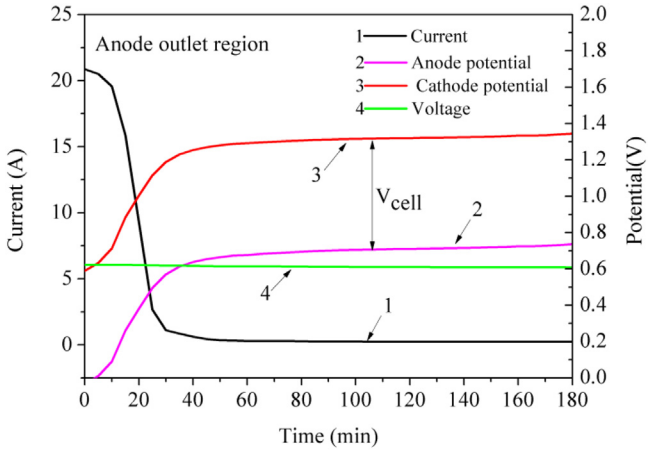

Fig. 6. Evolution of local potential and current at the anode outlet region.

the relative humidity of 80%. The operating temperature was kept at 60 °C. The constant voltage setting in the load was 0.6 V. The pure hydrogen (99.999%) and clean air were employed as the fuel and oxidant, respectively. The flow of the reactant gases were in a counter flow mode (see Fig. 1).

Fig. 4 depicts the variation of local current distribution during the DEA operation in a cycle. The current degrades firstly at segment 1 near the anode outlet, and then extends to the region near the inlet. That is because when operating with a DEA both convection and diffusion influence the distribution of gasses along the channel; and convection dominates the transfer process at the channel inlet, pushing gas phase towards the end of the anode, resulting in the appearing of the hydrogen depleted region (HDR) firstly at the anode outlet region (segment 1). Then the HDR will grow along the channel to the inlet, due to the parasitic gases (nitrogen and water vapor) accumulation [7].

In addition, the current of each segment except 1 reaches its maximum before the decline, as shown in Fig. 4. One reason may be that there is the electrical resistance R in the external circuit, which shares the output voltage of fuel cells U_{cell} with the load U_{Load} by potentiostatic control, as expressed below:

$$U_{cell} = U_{Load} + U_R \quad (1)$$

When the concentration of hydrogen is decreased gradually with a DEA, the total current is reduced, leading to the decline of the voltage U_R. From Eq. (1), it will lower the output voltage of fuel cells U_{cell}. By the effect of polarization, the reduced U_{cell} will cause the increased current in the subcell until lack of hydrogen, as indicated in Fig. 4.

3.2. Local potential distribution

Figs. 5 and 6 depict the variations of the local potentials and the local currents at the anode inlet and outlet regions during the DEA operation in a cycle. With the abundant supply of hydrogen at the anode inlet region, there are no obvious declines of both potential and current as shown in Fig. 5. However, the current distribution appears uneven obviously. The local current at the anode inlet ascends higher, while at the same time, the one at the anode outlet descends from 21 A to 0 A by comparing the two figures. It attributes to the oxygen and nitrogen permeation through the membrane from the cathode and the accumulation at the HDR with a DEA. Thus, the front of $N_2 + O_2/H_2$ is created [10], which leads to a high local cathode potential 1.34 V vs. DHE in Fig. 6 [11–13].

Under such a high potential, the carbon corrosion at the cathode side was accelerated corresponding to the hydrogen outlet region, as indicated by scanning electron microscope (SEM) in Fig. 7. The average thickness of cathode catalyst layer at the hydrogen inlet region is approximately 21.3 μm in Fig. 7a$_1$, while the one at the

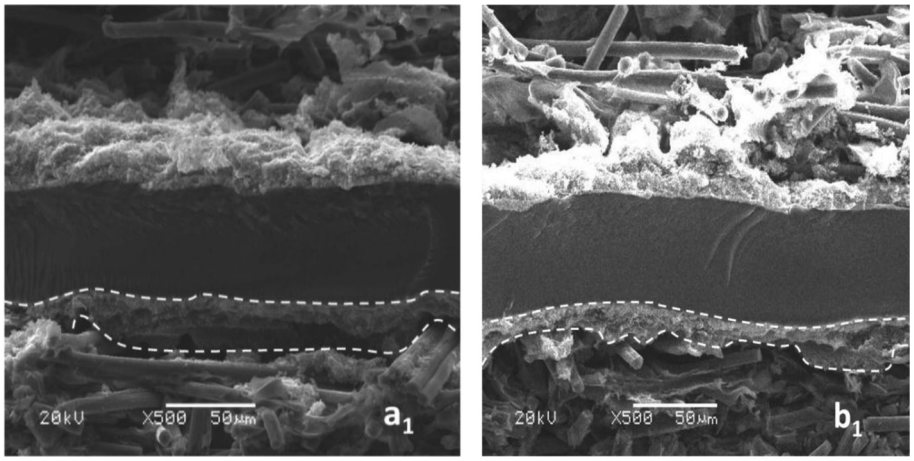

Fig. 7. The SEM images showing thickness (highlighted by white dotted lines) of the cathode electrodes (a_1 near the anode inlet and b_1 near the anode outlet). "a_2" and "b_2" is high magnification (200,000) showing morphology of cathode electrodes.

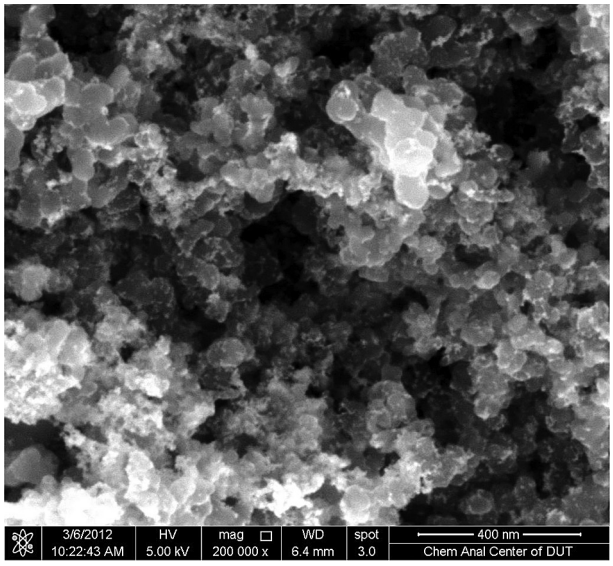

Fig. 8. The high-magnification (200,000) SEM image of the cathode electrodes near the anode inlet.

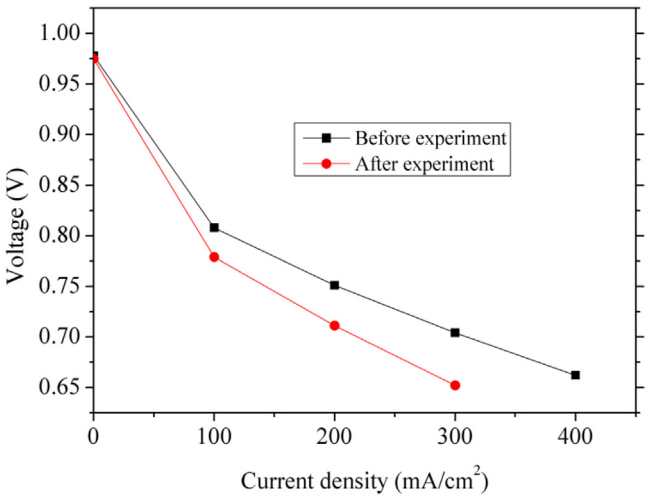

Fig. 10. The polarization curve before and after the continuously operation with a DEA (The cathode adopted the flow-through mode with P_C = 50 kPa, T_{cell} = 60 °C, RH_C = 80%, and λ_C = 2.5. Dry hydrogen was supplied to the anode at 50 kPa by an upstream pressure regulator during the DEA operation).

hydrogen outlet region is approximate 16.1 μm in Fig. 7b$_1$, as reported earlier in Ref. [14]. Figs. 8 and 9 are the related high-magnification SEM images, respectively. The pore structure of the GDL collapses obviously, which could be resulted from the carbon corrosion under the high potential. Both of the thickness reduction and the pore collapse of the GDL can lead to irreversible performance degradation seriously. The comparison of the performances before and after the DEA operation is given in Fig. 10. The performance declined rapidly after the continuously 180 min operation with a DEA.

3.3. Influence of nitrogen and water crossover on the performance of a PEMFC

The accumulations of the nitrogen and water vapor are the two major causes for the performance decline with a DEA in a short period. In order to distinguish which factor plays a major role on the performance in the short-term, the experiments are designed by using air (79% nitrogen and 21% oxygen) or oxygen (99.999%) as an oxidant and using high-purity hydrogen (99.999%) or a mixture of 99.2% hydrogen and 0.8% nitrogen as the fuel. The purge interval was controlled as a key parameter to investigate the influence on the performance in the short-term. The purge interval was determined by the automatic software which controlled the solenoid valve. The pure process was trigged by detecting the voltage loss (about 5% of its normal level) for all operation conditions. When the cell voltage recovered higher than the setting value, the valve would be back to the closed state. The longer the purge interval was, the slower the rate of decline would be.

From Fig. 11, when the high-purity hydrogen and high-purity oxygen were employed as the fuel and oxidant respectively, there is almost no potential loss for more than 120 min. However, when the high-purity and air are used, the purge intervals become shorter, approximately 40 min, 50 min, and 60 min at the current densities of 500, 300, and 100 mA cm^{-2}, respectively. The load and

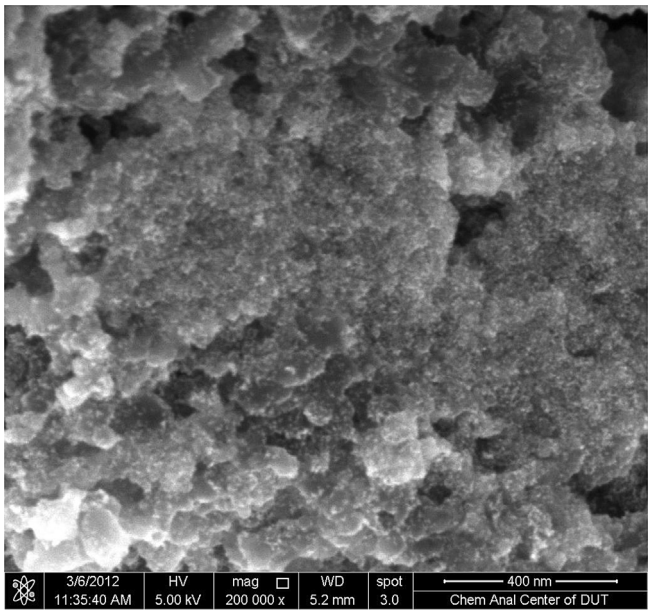

Fig. 9. The high-magnification (200,000) SEM image of the cathode electrodes near the anode outlet.

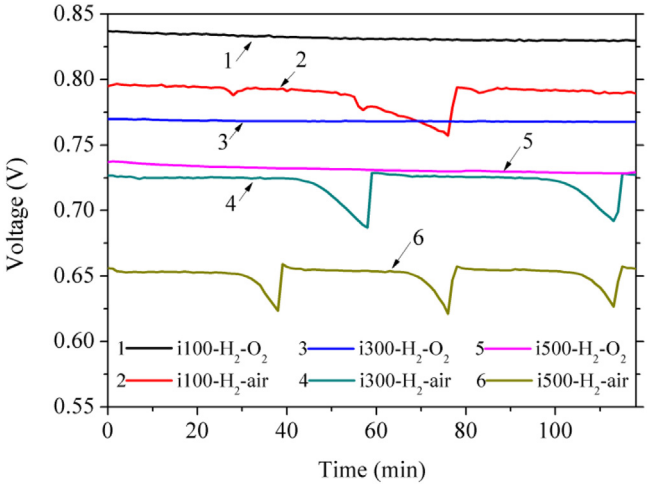

Fig. 11. Variation of cell voltages for the oxidants with various oxygen concentrations in the cathode ($P_A = P_C$ = 50 kPa, T_{cell} = 60 °C, RH_C = 80%, λ_C = 2.5).

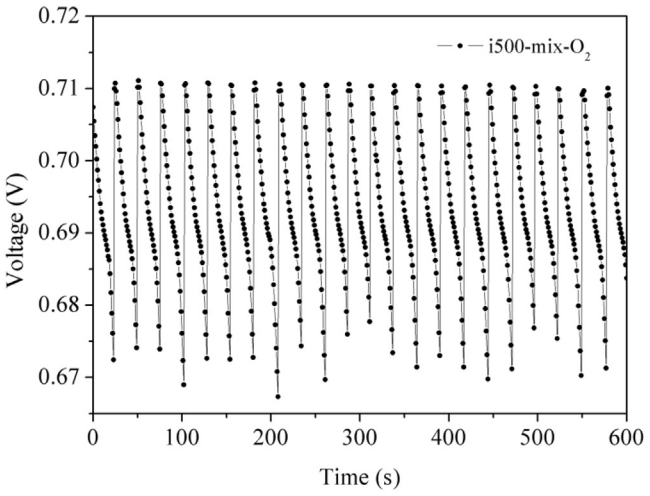

Fig. 12. Variation of cell voltages with the mixture (99.2% hydrogen and 0.8% nitrogen) as the fuel ($P_A = P_C = 50$ kPa, $T_{cell} = 60$ °C, $RH_C = 80\%$, $\lambda_C = 2.5$, $i = 500$ mA cm^{-2}).

the other operating conditions were kept consistent, while the purge intervals were much shorter when applied air instead of oxygen as the oxidant. It indicates nitrogen plays the main role on the performance decline in the testing period. Thus, the reduction of nitrogen concentration in cathode gas will be helpful for preventing the performance decline under the DEA operation. Yesilyurt et al. [15] also obtained the similar observation through studying the effect of the oxygen-to-nitrogen in the cathode on the voltage transients in the DEA operation with a time-dependent one-dimensional model.

Further, another experiment was designed to explain the role of nitrogen in the purge intervals. The mixture of 99.2% hydrogen and 0.8% nitrogen was used as the fuel and the high-purity oxygen was used as the oxidant, respectively. The current density was kept at 500 mA cm^{-2}. Then the response voltages were recorded with the time, as shown in Fig. 12. Although the H_2 concentration was only reduced from 99.999% to 99.2%, the purge intervals were sharply cut from more than 120 min (Fig. 11) to 25 s (Fig. 12). Thus, the experiment further indicates that the dominant factor on the potential loss would be the nitrogen crossover rather than the water accumulation in the anode channel in the short-term.

4. Conclusions

In this work, the evolutions of the local properties with a DEA have been studied by online monitoring the current distribution and the local potentials. Results indicate that the fuel distribution in the anode channels is uneven and time-varying during the DEA operation in a cycle. Due to the accumulation and crossover of water and nitrogen gas, the current firstly degrades at segment 1 near the anode outlet, and then proceeds to the region near the inlet. The local fuel starvation at the HDR results in a high cathode potential (1.34 V), which accelerates the carbon corrosion at the cathode side. The SEM images indicate that the significant thickness reduction and the pore collapse occur at the cathode electrode at the HDR near the anode outlet, which lead to the irreversible performance decline. Further, the experiments with different oxidants and fuels reveal that the dominant factor on the performance decay is the nitrogen crossover rather than the water accumulation in the anode in the short-term.

Acknowledgments

This work was financially supported by the “973” and “863” national key projects of nos. 2012CB215500 and 2011AA11A273.

References

[1] Yongtaek Lee, Bosung Kim, Yongchan Kim, Int. J. Hydrogen Energy 34 (2009) 7768–7779.
[2] Kyung Don Baik, Min Soo Kim, Int. J. Hydrogen Energy 36 (2011) 732–739.
[3] Agus P. Sasmito, Arun S. Mujumdar, Int. J. Hydrogen Energy 36 (2011) 10917–10933.
[4] Jason B. Siegel, Denise A. McKay, Anna G. Stefanopoulou, Daniel S. Hussey, David L. Jacobsonb, J. Electrochem. Soc. 155 (11) (2008) B1168–B1178.
[5] Jason B. Siegel, Stanislav V. Bohac, Anna G. Stefanopoulou, Serhat Yesilyurtc, J. Electrochem. Soc. 157 (7) (2010) B1081–B1093.
[6] W.R. Baumgartner, P. Parz, S.D. Fraser, E. Wallnofer, V. Hacker, J. Power Sources 182 (2008) 413–421.
[7] Jixin Chen, Jason B. Siegel, Toyoaki Matsuura, Anna G. Stefanopoulou, J. Electrochem. Soc. 158 (9) (2011) B1164–B1174.
[8] Dong Liang, Qiang Shen, Ming Hou, Zhigang Shao, Baolian Yi, J. Power Sources 194 (2009) 847–853.
[9] Zyun Siroma, Ryou Kakitsubo, Naoko Fujiwara, Tsutomu Ioroi, Shin-Ichi Yamazaki, Kazuaki Yasuda, J. Power Sources 156 (2006) 284–287.
[10] Q. Shen, M. Hou, D. Liang, Z. Zhou, X. Li, Z. Shao, B. Yi, J. Power Sources 189 (2009) 1114–1119.
[11] M. Farooque, A. Kush, L. Christner, J. Electrochem. Soc. 137 (7) (1990) 2025–2030.
[12] Jeremy P. Meyers, Robert M. Darling, J. Electrochem. Soc. 153 (8) (2006) A1432–A1442.
[13] Carl A. Reiser, Lawrence Bregoli, Timothy W. Patterson, Jun S. Yi, J. Delaing Yang, Mike L. Perry, Thomas D. Jarvi, Electrochem. Solid-State Lett. 8 (6) (2005) A273–A276.
[14] Toyoaki Matsuura, Jason B. Siegel, Jixin Chen, Anna G. Stefanopoulou, Proceedings of the ASME FuelCell2011, Aug. 7–10, Washington, DC.
[15] Serhat Yesilyurt, Jason B. Siegel, Anna G. Stefanopoulou, J. Fuel Cell Sci. Technol. 9 (2) (2012) 021012–021017.